

1 Crystal Structure of the Extended-Spectrum β -Lactamase PER-2 and Insights into the Role of
2 Specific Residues in the Interaction with β -Lactams and β -Lactamase Inhibitors.

3

4 Melina Ruggiero,¹ Frédéric Kerff,² Raphaël Herman,² Frédéric Sapunarić,² Moreno Galleni,²
5 Gabriel Gutkind,¹ Paulette Charlier,² Eric Sauvage,² Pablo Power^{1#}

6

7 Laboratorio de Resistencia Bacteriana, Facultad de Farmacia y Bioquímica, Universidad de
8 Buenos Aires, Argentina¹; Centre d'Ingénierie des Protéines, Université de Liège, Liège,
9 Belgium²

10

11 Running Head: Crystal Structure of the Class A β -Lactamase PER-2

12

13 [#] Address correspondence to Pablo Power, ppower@ffyb.uba.ar

14 **Abstract:**

15

16 PER-2 belongs to a small (7 members to date) group of extended-spectrum β -lactamases. It has
17 88% amino acid identity with PER-1 and both display high catalytic efficiencies towards most β -
18 lactams. In this study, we determined the X-ray structure of PER-2 at 2.20 Å, and evaluated the
19 possible role of several residues in the structure and activity towards β -lactams and mechanism-
20 based inhibitors. PER-2 is defined by the presence of a singular *trans* bond between residues
21 166-167 that generates an inverted Ω loop, and an expanded fold of this domain that results in a
22 wide active site cavity that allows for an efficient hydrolysis of antibiotics like the oxyimino-
23 cephalosporins, and a series of exclusive interactions between residues not frequently involved in
24 the stabilization of the active site in other class A β -lactamases. PER β -lactamases could be
25 included within a cluster of evolutionary related enzymes harboring conserved residues Asp136
26 and Asn179. Other signature residues that define these enzymes seem to be Gln69, Arg220,
27 Thr237, and probably Arg/Lys240A, with structurally important roles in the stabilization of the
28 active site and proper orientation of catalytic water molecules, among others. We propose,
29 supported by simulated models of PER-2 in combination with different β -lactams, the presence
30 of a hydrogen-bond network connecting Ser70-Gln69-Water-Thr237-Arg220 that might be
31 important for the proper activity and inhibition of the enzyme. Therefore, we could expect that
32 mutations occurring in these positions will have impact in the overall hydrolytic behavior.

33 **Introduction:**

34

35 Class A β -lactamases (E.C. 3.5.2.6) are the most prevalent enzymes conferring high-level
36 resistance to β -lactam antibiotics among human pathogens. This molecular group comprises
37 enzymes that efficiently hydrolyze amino-penicillins and older (first and second generation)
38 cephalosporins, and are inhibited, to different extents, by mechanism-based β -lactamase
39 inhibitors like clavulanic acid, tazobactam and sulbactam. They also encompass several
40 extended-spectrum β -lactamases (ESBL) that widen their range of hydrolysable drugs to newer
41 β -lactams such as the oxyimino-cephalosporins like cefotaxime (CTX) and ceftazidime (CAZ)
42 (1, 2).

43 Within the vast class A β -lactamases family, PER β -lactamases are a quite unique group of
44 ESBL that are circumscribed to few locations around the world (2). PER-1 was first recognized
45 in a clinical bacterial strain isolated from a hospitalized patient in France; it was more recently
46 detected among other microorganisms in a handful of other countries, especially *Pseudomonas*
47 *aeruginosa* and *Acinetobacter baumannii* (2-6). Other closely related enzymes are PER-3, -4, -5
48 and -7 (2, 7).

49 PER-2 was detected for the first time in a *Proteus mirabilis* strain isolated in Argentina in 1989,
50 although it was at that time named as ARG-1 (8). Nevertheless, the gene sequence located on a
51 transferable plasmid was described as *bla*_{PER-2} in a ceftibuten-resistant *Salmonella* Typhimurium
52 isolate (9).

53 Since its first report, PER-2 has been found in other species and countries, although it is
54 particularly prevalent in Argentina and Uruguay (2), and have accounted for up to 10% and 5%
55 of the oxyimino-cephalosporin resistance in *K. pneumoniae* and *E. coli*, respectively (10). PER-

56 6, encoded in the chromosome of an environmental *Aeromonas allosaccharophila* isolate, is the
57 only variant close to PER-2, that may elucidate the evolutionary path of PER β -lactamases (11).
58 PER-2 shares 88% amino acid sequence identity with mature PER-1 and both of them display
59 high catalytic efficiencies (k_{cat}/K_m) towards most β -lactams, generally characterized by similar
60 values for both ceftazidime and cefotaxime, although for PER-2 they seem to be nearly one order
61 of magnitude higher than PER-1 (12, 13). PER-2 is also strongly inhibited by mechanism-based
62 inhibitors such as clavulanate and tazobactam (12).
63 The X-ray structure of PER-1 has been solved (14), and the role of different residues has also
64 been studied for this variant (13, 15).
65 In this study, we determined the X-ray structure of PER-2 at 2.2 Å, and evaluated the possible
66 role of several key residues in the structure and activity towards β -lactams and mechanism-based
67 β -lactamase inhibitors.

68 **Materials and methods:**

69

70 **Strains and plasmids:**

71 *Escherichia coli* TC9 is a trans-conjugant clone harboring the pCf587 plasmid, used as the
72 source of *bla*_{PER-2} gene (12). *Escherichia coli* Top10F' (Invitrogen, USA) and *Escherichia coli*
73 BL21(DE3) (Novagen, USA) were hosts for transformation experiments. Plasmid vectors
74 pGEM-T Easy Vector (Promega, USA) and kanamycin-resistant pET28a(+) (Novagen,
75 Germany) were used for routine cloning experiments and for enzyme's overproduction,
76 respectively.

77

78 **Molecular biology techniques:**

79 Plasmid DNA (pTC9) was extracted using the methodology described by Hansen-Olsen (16).
80 The PER-2 encoding gene was amplified by PCR from plasmid pTC9, using 1 U Pfu DNA
81 polymerase (Promega, USA) and 0.4 μM PER2-BamF1 (5'-
82 TCATTTGTAGGATCCGCCCAATC-3') and PER2-SacR1 primers (5'-
83 CTTTAAGAGCTCGCTTAGATAGTG-3'), containing the *Bam*HI and *Sac*I restriction sites,
84 respectively (underlined in the sequences), designed for allowing the cloning of the mature PER-
85 2 coding sequence. The PCR product was first ligated in a pGEM-T Easy vector; the insert was
86 sequenced for verification of the identity of the *bla*_{PER-2} gene and generated restriction sites, as
87 well as the absence of aberrant nucleotides. The resulting recombinant plasmid (pGEM-T/*bla*_{PER-}
88 2) was then digested with *Bam*HI and *Sac*I, and the released insert was subsequently purified and
89 cloned in the *Bam*HI-*Sac*I sites of a pET28a(+) vector. The ligation mixture was used to first
90 transform *E. coli* Top10F' competent cells, and after selection of recombinant clones, a second

91 transformation was performed in *E. coli* BL21(DE3) competent cells in LB plates supplemented
92 with 30 µg/ml kanamycin. Selected positive recombinant clones were sequenced for confirming
93 the identity of the *bla*_{PER-2} gene, from them the recombinant clone *E. coli* BL-PER-2-BS
94 harboring pET/*bla*_{PER-2} plasmid was used for protein expression experiments. The resulting
95 construct expresses a fusion peptide including mature PER-2 encoding gene plus an additional
96 sequence containing a 6×His tag and a thrombin cleavage site. DNA sequences were determined
97 at the GIGA facilities (Liege, Belgium). Nucleotide and amino acid sequence analysis were
98 performed by NCBI (<http://www.ncbi.nlm.nih.gov/>) and ExPASy (<http://www.expasy.org/>)
99 analysis tools.

100

101 **PER-2 production and purification:**

102 Overnight cultures of recombinant *E. coli* BL-PER-2-BS (harboring pET/*bla*_{PER-2} plasmid
103 construction) were diluted (1/50) in 2 L LB containing 30 µg/ml kanamycin and grown at 37°C
104 until ca. 0.8 OD units ($\lambda = 600$ nm). In order to induce β -lactamase expression, 0.4 mM IPTG
105 was added and cultures were grown at 37°C for 3 hrs. After centrifugation at 8,000 rpm (4°C) in
106 a Sorvall RC-5C, cells were resuspended in sodium phosphate buffer (20 mM, pH 8.0),
107 supplemented with 3 U/ml benzonase (Sigma-Aldrich, USA), and crude extracts were obtained
108 by mechanic disruption in an EmulsiFlex-C3 homogenizer (Avestin Europe GmbH, Germany)
109 after three passages at 1,500 bar. After clarification by centrifugation at 12,000 rpm (4°C), clear
110 supernatants containing the PER-2 fusion peptide were filtrated by 1.6 and 0.45 µm pore size
111 membranes prior purification. Clear supernatants were loaded onto 5-mL HisTrap HP affinity
112 columns (GE Healthcare Life Sciences, USA), connected to an ÄKTA-purifier (GE Healthcare,
113 Uppsala, Sweden), and equilibrated with buffer A: 20 mM sodium phosphate buffer (pH 8.0), 0.5

114 M sodium chloride. The column was extensively washed to remove unbound proteins, and β -
115 lactamases were eluted with a linear gradient (0-100%; 2 ml/min flow rate) of buffer B: buffer A
116 + 500 mM imidazole, pH 8.0. Eluted fractions were screened for β -lactamase activity during
117 purification by an iodometric system using 500 μ g/ml ampicillin as substrate (17), and followed
118 by SDS-PAGE in 12% polyacrylamide gels. Active fractions were dialyzed against buffer A2
119 (20 mM Tris-HCl buffer, pH 8.0), and the HisTag was eliminated by thrombin digestion (16 hs
120 at 25°C), using 5U thrombin (Novagen, USA) per mg protein for complete proteolysis. Digestion
121 mixture was then loaded onto 1-mL HisTrap HP columns (GE Healthcare Life Sciences, USA)
122 equilibrated in buffer A2, and the pure mature PER-2 was separated from the digested histidine-
123 tagged peptide eluted with buffer B2 (buffer A2 + 500 mM imidazole, pH 8.0). Protein
124 concentration and purity were determined by the BCA-protein quantitation assay (Pierce,
125 Rockford, IL, US) using bovine serum albumin as standard, and by densitometry analysis on
126 15% SDS-PAGE gels, respectively. Purified protein was subjected to automatic Edman
127 degradation for the N-terminal amino acid sequence determination using an Applied Biosystems
128 492 Protein Sequencer (Perkin Elmer, Waltham, MA, US).

129

130 **Crystallization:**

131 Crystals were grown at 20°C using the hanging drop vapor diffusion method with drops
132 containing 2.5 μ L of PER-2 solution (3.5 mg/mL), 1 μ L 0.1 M HEPES, in 1.5 M sodium citrate
133 buffer (pH 7.5), equilibrated against 1 mL of the latter solution at 20 °C.

134

135 **Data collection and phasing:**

136 Data were collected on a Pilatus 6M Dectris detector at a wavelength of 0.98011 Å on Proxima 1
137 beamline at the Soleil Synchrotron (Saint Aubin, France). X-Ray diffraction experiments were
138 carried out under cryogenic conditions (100°K) after transferring the crystals into cryo-protectant
139 solution containing 1.8 M ammonium sulfate and 45% (v/v) glycerol. Indexing and integration
140 were carried out using XDS (18), and the scaling of the intensity data was accomplished with
141 XSCALE (19).

142

143 **Model building and refinement:**

144 Refinement of the model was carried out using REFMAC5 (20), TLS (21), and Coot (22).
145 Models visualization and representation were performed with PyMol (www.pymol.org) (23).
146 The structure of PER-2 was refined to 2.2 Å, and deposited at the Protein Data Bank under
147 accession code 4D2O.

148

149 **Simulated modeling of PER-2 in complex with oxyimino-cephalosporins and clavulanate:**

150 The X-ray structure of PER-2 was used to model acyl-enzyme structures with ceftazidime,
151 cefotaxime and clavulanic acid. The structures with PDB id code 2ZQD (TOHO-1 in complex
152 with ceftazidime), 1IYO (TOHO-1 in complex with cefotaxime (24)) and 2H0T (SHV-1 in
153 complex with clavulanic acid (25)) were used for initial positioning of each ligand in PER-2
154 structure. Simulation structures were energy minimized with the program Yasara (26), using a
155 standard protocol consisting in a steepest descent minimization followed by simulated annealing
156 of the ligand and protein side chains. PER-2 backbone atoms were kept fixed during the whole
157 procedure. Simulation parameters consisted in the use of Yasara2 force field (27), a cutoff

158 distance of 7.86 Å, particle mesh Ewald (PME) long range electrostatics (28), periodic boundary
159 conditions and water filled simulation cell.

160 **Results and Discussion:**

161

162 **Structure determination of PER-2 β -lactamase:**

163 The structure of PER-2 was obtained at a resolution of 2.2 Å. Main data and refinement statistics
164 are given in Table 1.

165 The refined structure consists in two monomers per asymmetric unit. Monomer A includes 280
166 amino acids of mature β -lactamase, from Ala24 to Val297; monomer B contains 278 residues,
167 from Ser26 to Val297. The structure is solvated by 152 ordered water molecules.

168 The electron density map is well defined along the main chain of both monomers except for the
169 region covering residues Leu103-Gln103A-Asn103B in chain A, and the last C-terminal residues
170 (Ser298-Pro299-Asp300) in both chains.

171 The rms deviation between the equivalent C α atoms in both monomers is 0.64 Å and no
172 significant difference is found between the two active sites. Due to this observation, the
173 following discussion will refer to both monomers unless otherwise noted.

174

175 **PER-2 and PER-1 share the overall structure and main structural features within the**
176 **active site:**

177 The overall fold of the native PER-2 β -lactamase is similar to the previously reported PER-1
178 structure (PDB: 1E25) (14), displaying a rmsd of 0.619 Å between them.

179 As other class A β -lactamases, the active site motifs are located in the interface between the “all
180 α ” and “ α/β ” domains. They are defined as “Ser70-Val71-Phe72-Lys73” (motif 1, carrying the
181 nucleophile serine), “Ser130-Asp131-Asn132” (motif 2, in the loop between α 4 and α 5), and

182 “Lys234-Thr235-Gly236” (motif 3, on strand β 3), and the 14-residues-long Ω -loop, from Ala164
183 to Asn179 (Figure 1).

184 Compared to other class A β -lactamases, there are three insertions along the sequence of PER-2:
185 (i) Gln103A-Asn103B, and (ii) Gln112A-Gly112B, both located at the bottom of the “all α ”
186 domain, as part of a long fold connecting helices α 2 and α 4, and facing the Ω loop; and (iii)
187 Arg240A-Ala240B-Gly240C-Lys240D insertion that creates an enlarged loop just after the
188 “KTG” conserved motif (Figure 2a).

189 The insertion Gln103A-Asn103B creates a new fold that seems to be stabilized by hydrogen
190 bonds between Ser106 backbone and probably some rotamers of Gln103B, which is different to
191 the conserved bend (Val103-Asn106) in other class A β -lactamases like the CTX-M (24).

192 The most relevant structural trait observed in PER-2 (and also PER-1 (14)) is the presence of an
193 expanded active site, which would contribute to a facilitated access of bulkier molecules such as
194 the oxyimino-cephalosporins. This is achieved by two main features: a unique “inverted” Ω loop
195 (Figure 2a), whose configuration is the result of a *trans* bond between Glu166 and Ala167
196 (instead of the normally occurring *cis* bond in all the other class A β -lactamases), and an
197 expanded loop between the β 3 and β 4 strands (named β 3- β 4 loop) resulting from the insertion of
198 four-residues after the “KTG” motif that enlarges the active site entrance up to 12.2 Å (compared
199 to *ca* 6.5 Å in other class A β -lactamases) (Figure 2b).

200 The overall structure of the Ω loop is stabilized by hydrogen bonds between the carboxylate’s
201 oxygen of Asp136 (replacing the highly conserved Asn136 in other class A β -lactamases) and
202 main chain nitrogen atoms of Glu166 (2.9 Å) and Ala167 (3.0 Å) (Figure 2c), and by additional
203 bonds between Ala164 and Asn179, the initial and final residues of the Ω loop.

204 The positioning and orientation of side chains of important residues as Ser70, Lys73, Ser130,
205 Glu166 and Thr237 is equivalent to other class A β -lactamases (Figure 3a and 3b). These
206 findings, and the fact that C α -rmsd values of the conserved motifs of PER-2 compared to other
207 class A β -lactamases indicate that there is conservation in the overall structure of the active site
208 (Table 2).

209 The presence of a water molecule associated with the oxyanion hole (Wat14 in monomer A,
210 Wat113 in monomer B) is noticed (Figure 3a); it is located at 3.29 Å and 2.85 Å from the
211 oxyanion hole's Ser70N and Thr237N, respectively (Figure 3b), in agreement to the proposed
212 water molecule found at the PER-1 active site (Wat2153) (14) and other class A β -lactamases as
213 well (for reference, see PDB molecules 1BTL: TEM-1; 1SHV: SHV-1; 1IYS: TOHO-1; KPC-2:
214 3DW0).

215 On the other hand, the presence of a deacylating water is not clearly evidenced; no electron
216 density is apparent at equivalent position of the deacylating water Wat2075 in PER-1 (14).

217

218 **Additional structural features probably involved in the stabilization of the active site of**
219 **PER-2:**

220 We observed several features at the active site's environment of PER-2 not previously evaluated
221 for PER-1 (some of them are shown in Figure 3a).

222 A water molecule (Wat52) at the entrance of the catalytic site stabilizes the sharp β 3- β 4 fold
223 through hydrogen bonds with residues of the Ω loop, probably avoiding possible clashes between
224 both domains.

225 Some of the possible rotamers of Arg240A (at the end of the β 3 strand, replaced by Lys240A in
226 PER-1) could interact with Asp173 (at the Ω loop), probably modulating the rate by which β -
227 lactams gain access to the active site (see below).

228 The benzyl side chain of Phe72 rotates *ca* 45° relative to the same residue in other class A β -
229 lactamases like TEM and SHV (CTX-M enzymes contain a serine at position 72), creating a
230 hydrophobic environment (due to repulsion between Phe72 and Phe139) that could have an
231 impact on the interaction with some antibiotics. Alternatively, Met169 (replaced by leucine in
232 other class A β -lactamases) could induce the Phe72 rotation by non-hydrogen bond interactions
233 (29, 30).

234

235 **Gln69, Arg220 and Thr237 participate in a hydrogen-bond network important for the**
236 **stabilization of the active site:**

237 Previous studies have already scrutinized the role of different residues in the ability of PER-1 to
238 hydrolyze third-generation cephalosporins (13, 15). The influence of other residues in the
239 inhibition by mechanism-based inhibitors has been also assessed (31).

240 Glutamine 69 has been proposed as the second ligand for the deacylating water for PER-1 (14),
241 homologous to Asn170 in the other class A β -lactamases (32, 33). We observed that Gln69 side
242 chain in PER-2 seems to occupy equivalent space than the highly conserved Asn170 from other
243 class A β -lactamases like TOHO-1. This is partly due to the fact that Asn170 is replaced by
244 His170 in PER enzymes, and its relative position to the active site's environment is dramatically
245 modified as the result of the peculiar Ω loop (C α of His170 is displaced between 6.5-7.3 Å away
246 from the active).

247 It is known that in class A β -lactamases like TEM and SHV variants, Arg244 seems to play an
248 important role in substrate and inhibitor binding (34-36). This role seems to be fulfilled in CTX-
249 M β -lactamases by Arg276 (37). In other class A β -lactamases like the *Streptomyces albus* G β -
250 lactamase, or KPC-2 and NMC-A carbapenemases (PDB entries 1BSG, 3DW0 and 1BUE,
251 respectively) (38), an arginine residue at position 220 was observed at β 4 strand whose side
252 chain's guanidinium group occupies equivalent position than lateral residue of Arg244/Arg276
253 in the mentioned class A β -lactamases. For some of these enzymes, Arg220 was evaluated
254 regarding its influence in the substrate and inhibitor's binding, giving this residue a similar role
255 than Arg244 in TEM/SHV variants (39, 40).

256 For PER-1, the same role has been suggested according to an Arg220Leu mutant showing
257 modified kinetic parameters towards some β -lactams (13).

258 In fact, we have structural evidences for supporting that Arg220 in PER-2 allows the creation of
259 a different network of interactions with neighboring residues in comparison with the associations
260 observed in β -lactamases harboring Arg244/276. As shown in Figure 3c, the guanidinium group
261 of Arg220 hydrogen bonds with Thr237 (2.7 and 2.8 Å), Asn245 (3.1 Å), Glu276 (2.7 Å), and
262 Gly236 (3.2 Å), and additional interactions occur between Arg220 and Gly217, Lys222, and
263 Gly223 (through hydrogen bonds), and between Arg220 side chain with Asp246 through non-
264 polar interaction. In TEM-1, SHV-1 and TOHO-1, fewer polar interactions occur between
265 Arg244/Arg276 and close residues (not shown), and these differences could partially explain the
266 higher catalytic efficiencies of PER-2 towards some antibiotics.

267 Another striking difference between PER β -lactamases and the vast majority of class A enzymes
268 is the presence of a threonine at position 237. From the structure of PER-2, we confirm that
269 Thr237 seems to be important for connecting essential residues of the active site with Arg220

270 through a not previously reported network of hydrogen bonds, comprising Ser70-Gln69-Wat14-
271 Thr237-Arg220, in which Thr237 could serve as a stake connecting both domains (Figure 3b),
272 and additional interactions between Arg220 with both Thr244 and Glu276 that could further
273 improve the overall stabilization of the structure. In fact, both Arg220 and Thr237 seem to
274 contribute to the topology's adjustment of the oxyanion pocket, as also suggested for other class
275 A β -lactamases (13, 41). The hydroxyl group of Thr237 is also important for the interaction with
276 the substrate, providing the possibility for an additional hydrogen bond with the substrate's
277 carboxylate group, as described below.

278

279 **Simulated acyl-enzyme models of PER-2 could bring some clues about the interaction with**
280 **oxyimino-cephalosporins and inhibitors:**

281 As seen in Figure 4a, using simulated acyl-enzyme model of PER-2 structure in complex with
282 cefotaxime (generated using TOHO-1/cefotaxime structure; PDB 1IYO (24)), cefotaxime is
283 positioned in the binding site of PER-2 through hydrogen bonds with Gln69, Ser130, Asn132,
284 Glu166, Thr235, and Thr237. Altogether, these interactions with cefotaxime molecule could
285 support the efficient hydrolysis of the oxyimino-cephalosporins by PER β -lactamases (11, 12,
286 15).

287 As discussed, Thr237 could be involved in a critical networking, by stabilizing the active site and
288 the β 3 strand, acting as a connector of the β -lactam molecule with Arg220, the other essential
289 residue in this network. From the model, we propose that Arg240A (present in the enlarged loop
290 connecting β 3 and β 4 strands), could be involved in some stage during the entrance of
291 cefotaxime in the active site, probably assisted by Asp173. In TOHO-1 and other class A β -
292 lactamases, Asp240 (at equivalent position than Arg240A in PER-2) participates in the

293 interaction with the aminothiazol ring of cefotaxime during entrance to the active site (24, 42),
294 although we don't have evidences of such an interaction between cefotaxime and Arg240A in
295 PER-2.

296 A similar scenario is obtained for the acylated PER-2 model in complex with ceftazidime (Figure
297 4b), using the TOHO-1/ceftazidime structure (2ZQD). The model predicts that the existence of
298 an expanded catalytic cavity could in fact allow a suitable accommodation of ceftazidime
299 through interactions with Gln69, Ser130, Asn132, Glu166, Thr235, and Thr237.

300 Additional interactions between ceftazidime and other residues were also detected in comparison
301 to other β -lactamases. For example, Asp173, Gln176 and Arg240A seem to be closer to the
302 ceftazidime molecule and could have some role in the accommodation or entrance of the
303 molecule. In addition, the dihydrothiazine ring in the ceftazidime molecule allows van der Waals
304 interactions with Trp105, and the long carboxy-propoxyimino group could probably establish
305 additional polar interactions with Thr237 and Ser238 carbonyl oxygen atoms, which is probably
306 due to the increased flexibility in the PER-2 β 3 strand. Supporting this hypothesis, Ser238 is
307 involved in the efficient hydrolysis of ceftazidime in TEM/SHV ESBLs, by advantageous
308 interactions with Ser238 and Asn170 (the spatial equivalent to Gln69 in PER enzymes) (43). In
309 CTX-M β -lactamases, the low hydrolysis rate of ceftazidime could be explained by unfavorable
310 interactions or even repulsion between active site residues and the ceftazidime's carboxy-
311 propoxyimino group in the C7 β side chain (44).

312 Therefore, the interactions predicted between PER-2 and ceftazidime might explain the observed
313 high catalytic efficiencies of PER β -lactamases towards ceftazidime (12, 13, 15). The observed
314 differences in the kinetic behavior towards ceftazidime between PER-2 and PER-1 could be

315 probably due to the presence of differential residues like Arg240A (replaced by Lys in PER-1),
316 and deserve further studies.

317 Finally, inactivators like clavulanic acid could be also properly stabilized during inhibition (data
318 not shown), based on models obtained by comparison with the structure of SHV-1 in complex
319 with clavulanate (PDB 2H0T) (45). According to the models, Gln69, Arg220, Thr237 and
320 probably Arg240A could be important in the stabilization of the clavulanate molecule.

321 In TEM and SHV β -lactamases with decreased susceptibility to inhibition by clavulanic acid,
322 various mutations at Arg244 suggest that the interaction between this residue and the clavulanate
323 carboxylate is essential for clavulanate-mediated inactivation (35, 38, 46, 47).

324 In a recent publication, it was shown that clavulanate, upon acylation of the class A β -lactamase
325 from *Bacillus licheniformis* BS3, generates two moieties, named CL1 (covalently linked to
326 Ser70) and CL2 (48). According to comparative models with PER-2, both fragments could be in
327 part associated by hydrogen bonds with residues like Gln69, Ser70, Ser130 and Thr237 (data not
328 shown), if a similar inactivation mechanism actually occurs.

329 It has been previously reported that mutations at Gln69 do not seem to impair the inactivation by
330 clavulanate (31). In addition, replacement of Arg220 or Thr237 seem to alter the behavior of
331 PER-1 towards cephalosporins (13).

332 Preliminary results with different mutants of PER-2 in Arg220 have shown that modifications in
333 this residue not only affect the susceptibility to inhibitors but also seem to impact the catalytic
334 behavior towards several antibiotics, especially cephalosporins (49).

335 As these residues appear to be important for the stabilization of the oxyanion pocket, mutations
336 in either of these residues could probably affect the proper inactivation by mechanism-based

337 inhibitors, probably by breaking the integrity of the conserved hydrogen-bonds network in which
338 they participate.

339

340 **Conclusions:**

341

342 Extended-spectrum β -lactamase PER-2 is a unique enzyme from a structural point of view,
343 belonging to a still small and not widely disseminated group of β -lactamases (seven members are
344 recognized nowadays) in which PER-1 and PER-2 represent the more frequently detected
345 members.

346 We provided herein structural evidences of PER-2 suggesting that a previously not described
347 hydrogen-bond network connecting Ser70-Gln69-Water-Thr237-Arg220 is essential for the
348 proper activity and inhibition of the enzyme.

349 We have also presented, through simulated models of PER-2 in association with oxyimino-
350 cephalosporins and clavulanate, the first evidences on the probable interactions of these β -
351 lactams with key residues of the active site, proposing that residues like Gln69, Arg220, Thr237,
352 and probably Asp173 and Arg240A are important for the accommodation of β -lactams within the
353 active site, and their entrance, respectively.

354 Our results could serve to catch a glimpse of hypothetically emerging mutants having disrupted
355 hydrogen-bond networks that would display lower catalytic efficiencies towards some β -lactams
356 (especially cephalosporins) and poorer inhibition by clavulanic acid.

357 Further real structural models, complemented by kinetic data, will give us a more thoughtful idea
358 about the actual role of these residues in the high catalytic efficiency of PER-2 towards most β -
359 lactams. In this regard, we foresee that mutations in either Arg220 (the counterpart of Arg244 in

360 TEM/SHV variants) or Thr237 would probably result in more dramatic changes in the kinetic
361 activity.

362 **Acknowledgments:**

363

364 This work was supported by grants from the University of Buenos Aires (UBACyT 2012-2015 to
365 PP; and 2011-2014 to GG), Consejo Nacional de Investigaciones Científicas y Técnicas
366 (CONICET PIP 2010-2012 to PP), Agencia Nacional de Promoción Científica y Tecnológica
367 (BID PICT 2011-0742 to GG), the Fonds de la Recherche Scientifique (IISN 4.4505.09, IISN
368 4.4509.11, FRFC 2.4511.06F), by the Belgian Program on Interuniversity Poles of Attraction
369 initiated by the Belgian State, Prime Minister's Office, Science Policy programming (IAP no.
370 P6/19, P7/44), by the University of Liège (Fonds spéciaux, Crédit classique, C-06/19 and C-
371 09/75), and by a bilateral scientific agreement (V4/325C) between the Belgian Funds for
372 Scientific Research (FRS-FNRS) to MG and the Consejo Nacional de Investigaciones Científicas
373 y Técnicas (CONICET) to GG and later to PP.

374 M. Ruggiero is a PhD fellow for the Consejo Nacional de Investigaciones Científicas y Técnicas
375 (CONICET, Argentina), and was a recipient of an Alfa-Bacterialnet Doctoral visiting fellowship
376 at the CIP (U. Liege). P. Power and G. Gutkind are researchers for the CONICET, Argentina. F.
377 Kerff is an associate researcher for the Fonds de la Recherche Scientifique (FNRS, Belgium).

378 We thank the staff of Proxima1 beamline at Soleil synchrotron for assistance in X-ray data
379 collection, and Nicole Otthiers, Anne-Marie Matton and Fabrice Bouillenne (CIP, University of
380 Liege, Belgium) for precious assistance in the N-terminal determination and β -lactamase
381 purification process.

382 **References:**

383

384 1. **Bush K, Jacoby GA.** 2010. Updated functional classification of β -lactamases. *Antimicrob.*
385 *Agents Chemother.* **54**:969-976.

386 2. **Gutkind GO, Di Conza J, Power P, Radice M.** 2013. β -Lactamase-mediated resistance: a
387 biochemical, epidemiological and genetic overview. *Curr. Pharm. Des.* **19**:164-208.

388 3. **Nordmann P, Ronco E, Naas T, Duport C, Michel-Briand Y, Labia R.** 1993. Characterization
389 of a novel extended-spectrum β -lactamase from *Pseudomonas aeruginosa*. *Antimicrob. Agents*
390 *Chemother.* **37**:962-969.

391 4. **Vahaboglu H, Dodanli S, Eroglu C, Ozturk R, Soyletir G, Yildirim I, Avkan V.** 1996.
392 Characterization of multiple-antibiotic-resistant *Salmonella typhimurium* stains: molecular
393 epidemiology of PER-1-producing isolates and evidence for nosocomial plasmid exchange by a
394 clone. *J. Clin. Microbiol.* **34**:2942-2946.

395 5. **Vahaboglu H, Ozturk R, Aygun G, Coskuncan F, Yaman A, Kaygusuz A, Leblebicioglu H,**
396 **Balik I, Aydin K, Otkun M.** 1997. Widespread detection of PER-1-type extended-spectrum β -
397 lactamases among nosocomial *Acinetobacter* and *Pseudomonas aeruginosa* isolates in Turkey: a
398 nationwide multicenter study. *Antimicrob. Agents Chemother.* **41**:2265-2269.

399 6. **Poirel L, Karim A, Mercat A, Le Thomas I, Vahaboglu H, Richard C, Nordmann P.** 1999.
400 Extended-spectrum β -lactamase-producing strain of *Acinetobacter baumannii* isolated from a
401 patient in France. *J. Antimicrob. Chemother.* **43**:157-158.

402 7. **Bonnin RA, Potron A, Poirel L, Lecuyer H, Neri R, Nordmann P.** 2011. PER-7, an extended-
403 spectrum β -lactamase with increased activity toward broad-spectrum cephalosporins in
404 *Acinetobacter baumannii*. *Antimicrob. Agents Chemother.* **55**:2424-2427.

- 405 8. **Rossi MA, Gutkind G, Quinteros M, Marino E, Couto E, Tokumoto M, Woloj M, Miller G,**
406 **Medeiros A.** 1991. A *Proteus mirabilis* with a novel extended spectrum β -lactamase and six
407 different aminoglycoside resistance genes, abstr 939., p p 255. Abstr. 31st Intersc. Conf. on
408 Antimicrob. Agents & Chemother., Chicago, IL, USA.
- 409 9. **Bauernfeind A, Stemplinger I, Jungwirth R, Mangold P, Amann S, Akalin E, Ang O, Bal C,**
410 **Casellas JM.** 1996. Characterization of beta-lactamase gene *bla*_{PER-2}, which encodes an extended-
411 spectrum class A β -lactamase. Antimicrob. Agents Chemother. **40**:616-620.
- 412 10. **Quinteros M, Radice M, Gardella N, Rodríguez MM, Costa N, Korbenfeld D, Couto E,**
413 **Gutkind G, The Microbiology Study Group.** 2003. Extended-spectrum β -lactamases in
414 *Enterobacteriaceae* in Buenos Aires, Argentina, public hospitals. Antimicrob. Agents Chemother.
415 **47**:2864-2869.
- 416 11. **Girlich D, Poirel L, Nordmann P.** 2010. PER-6, an extended-spectrum β -lactamase from
417 *Aeromonas allosaccharophila*. Antimicrob. Agents Chemother. **54**:1619-1622.
- 418 12. **Power P, Di Conza J, Rodriguez MM, Ghiglione B, Ayala JA, Casellas JM, Radice M,**
419 **Gutkind G.** 2007. Biochemical characterization of PER-2 and genetic environment of *bla*_{PER-2}.
420 Antimicrob. Agents Chemother. **51**:2359-2365.
- 421 13. **Bouthors AT, Delettre J, Mugnier P, Jarlier V, Sougakoff W.** 1999. Site-directed mutagenesis
422 of residues 164, 170, 171, 179, 220, 237 and 242 in PER-1 β -lactamase hydrolysing expanded-
423 spectrum cephalosporins. Protein Eng. **12**:313-318.
- 424 14. **Tranier S, Bouthors AT, Maveyraud L, Guillet V, Sougakoff W, Samama JP.** 2000. The high
425 resolution crystal structure for class A β -lactamase PER-1 reveals the bases for its increase in
426 breadth of activity. J. Biol. Chem. **275**:28075-28082.

- 427 15. **Bouthors AT, Dagoneau-Blanchard N, Naas T, Nordmann P, Jarlier V, Sougakoff W.** 1998.
428 Role of residues 104, 164, 166, 238 and 240 in the substrate profile of PER-1 β -lactamase
429 hydrolysing third-generation cephalosporins. *Biochem. J.* **330**:1443-1449.
- 430 16. **Hansen JB, Olsen RH.** 1978. Isolation of large bacterial plasmids and characterization of the P2
431 incompatibility group plasmids pMG1 and pMG5. *J. Bacteriol.* **135**:227-238.
- 432 17. **Power P, Radice M, Barberis C, de Mier C, Mollerach M, Maltagliatti M, Vay C,**
433 **Famiglietti A, Gutkind G.** 1999. Cefotaxime-hydrolysing β -lactamases in *Morganella*
434 *morganii*. *Eur. J. Clin. Microbiol. Infect. Dis.* **18**:743-747.
- 435 18. **Kabsch W.** 2010. XDS. *Acta Crystallogr. D Biol. Crystallogr.* **66**:125-132.
- 436 19. **Kabsch W.** 2010. Integration, scaling, space-group assignment and post-refinement. *Acta*
437 *Crystallogr. D Biol. Crystallogr.* **66**:133-144.
- 438 20. **Murshudov GN, Vagin AA, Dodson EJ.** 1997. Refinement of macromolecular structures by the
439 maximum-likelihood method. *Acta Crystallogr D Biol Crystallogr* **53**:240-55.
- 440 21. **Painter J, Merritt EA.** 2006. Optimal description of a protein structure in terms of multiple
441 groups undergoing TLS motion. *Acta Crystallogr D Biol Crystallogr* **62**:439-50.
- 442 22. **Emsley P, Cowtan K.** 2004. Coot: model-building tools for molecular graphics. *Acta*
443 *Crystallogr. D Biol. Crystallogr.* **60**:2126-2132.
- 444 23. **Schrödinger L.** The PyMOL Molecular Graphics System., 1.5.0.4 ed.
- 445 24. **Shimamura T, Ibuka A, Fushinobu S, Wakagi T, Ishiguro M, Ishii Y, Matsuzawa H.** 2002.
446 Acyl-intermediate structures of the extended-spectrum class A β -lactamase, Toho-1, in complex
447 with cefotaxime, cephalothin, and benzylpenicillin. *J. Biol. Chem.* **277**:46601-46608.
- 448 25. **Padayatti PS, Helfand MS, Totir MA, Carey MP, Carey PR, Bonomo RA, van den Akker F.**
449 2005. High resolution crystal structures of the trans-enamine intermediates formed by sulbactam
450 and clavulanic acid and E166A SHV-1 β -lactamase. *J. Biol. Chem.* **280**:34900-34907.

- 451 26. **Krieger E, Darden T, Nabuurs SB, Finkelstein A, Vriend G.** 2004. Making optimal use of
452 empirical energy functions: force-field parameterization in crystal space. *Proteins* **57**:678-683.
- 453 27. **Krieger E, Joo K, Lee J, Raman S, Thompson J, Tyka M, Baker D, Karplus K.** 2009.
454 Improving physical realism, stereochemistry, and side-chain accuracy in homology modeling:
455 Four approaches that performed well in CASP8. *Proteins* **77**:114-122.
- 456 28. **Essmann U, Perera L, Berkowitz ML, Darden T, Lee H, Pedersen LG.** 1995. A smooth
457 particle mesh Ewald method. *J. Chem. Phys.* **103**:8577-8593.
- 458 29. **Pal D, Chakrabarti P.** 1998. Different types of interactions involving cysteine sulfhydryl group
459 in proteins. *J. Biomol. Struct. Dyn.* **15**:1059-1072.
- 460 30. **Tatko CD, Waters ML.** 2004. Investigation of the nature of the methionine- π interaction in β -
461 hairpin peptide model systems. *Protein Sci.* **13**:2515-2522.
- 462 31. **Bouthors AT, Jarlier V, Sougakoff W.** 1998. Amino acid substitutions at positions 69, 165, 244
463 and 275 of the PER-1 β -lactamase do not impair enzyme inactivation by clavulanate. *J.*
464 *Antimicrob. Chemother.* **42**:399-401.
- 465 32. **Chen CC, Herzberg O.** 1999. Relocation of the catalytic carboxylate group in class A β -
466 lactamase: the structure and function of the mutant enzyme Glu166-->Gln:Asn170-->Asp. *Protein*
467 *Eng.* **12**:573-579.
- 468 33. **Zawadzke LE, Chen CC, Banerjee S, Li Z, Wasch S, Kapadia G, Moulton J, Herzberg O.**
469 1996. Elimination of the hydrolytic water molecule in a class A β -lactamase mutant: crystal
470 structure and kinetics. *Biochem. J.* **35**:16475-16482.
- 471 34. **Bret L, Chaibi EB, Chanal-Claris C, Sirot D, Labia R, Sirot J.** 1997. Inhibitor-resistant TEM
472 (IRT) β -lactamases with different substitutions at position 244. *Antimicrob. Agents Chemother.*
473 **41**:2547-2549.

- 474 35. **Thomson JM, Distler AM, Prati F, Bonomo RA.** 2006. Probing active site chemistry in SHV
475 β -lactamase variants at Ambler position 244. Understanding unique properties of inhibitor
476 resistance. *J. Biol. Chem.* **281**:26734-26744.
- 477 36. **Moews PC, Knox JR, Dideberg O, Charlier P, Frere JM.** 1990. β -Lactamase of *Bacillus*
478 *licheniformis* 749/C at 2 Å resolution. *Proteins* **7**:156-171.
- 479 37. **Perez-Llarena FJ, Cartelle M, Mallo S, Beceiro A, Perez A, Villanueva R, Romero A,**
480 **Bonnet R, Bou G.** 2008. Structure-function studies of arginine at position 276 in CTX-M β -
481 lactamases. *J. Antimicrob. Chemother.* **61**:792-797.
- 482 38. **Marciano DC, Brown NG, Palzkill T.** 2009. Analysis of the plasticity of location of the Arg244
483 positive charge within the active site of the TEM-1 β -lactamase. *Protein Sci.* **18**:2080-2089.
- 484 39. **Jacob-Dubuisson F, Lamotte-Brasseur J, Dideberg O, Joris B, Frere JM.** 1991. Arginine 220
485 is a critical residue for the catalytic mechanism of the *Streptomyces albus* G β -lactamase. *Protein*
486 *Eng.* **4**:811-819.
- 487 40. **Papp-Wallace KM, Taracila MA, Smith KM, Xu Y, Bonomo RA.** 2012. Understanding the
488 molecular determinants of substrate and inhibitor specificity in the carbapenemase, KPC-2:
489 exploring the roles of Arg220 and Glu276. *Antimicrob. Agents Chemother.* **56**:4428-4438.
- 490 41. **Matagne A, Frere JM.** 1995. Contribution of mutant analysis to the understanding of enzyme
491 catalysis: the case of class A β -lactamases. *Biochim. Biophys. Acta* **1246**:109-127.
- 492 42. **Delmas J, Leyssene D, Dubois D, Birck C, Vazeille E, Robin F, Bonnet R.** 2010. Structural
493 insights into substrate recognition and product expulsion in CTX-M enzymes. *J. Mol. Biol.*
494 **400**:108-120.
- 495 43. **Raquet X, Lamotte-Brasseur J, Fonce E, Goussard S, Courvalin P, Frere JM.** 1994. TEM β -
496 lactamase mutants hydrolysing third-generation cephalosporins. A kinetic and molecular
497 modelling analysis. *J. Mol. Biol.* **244**:625-639.

- 498 44. **Ibuka AS, Ishii Y, Galleni M, Ishiguro M, Yamaguchi K, Frere JM, Matsuzawa H, Sakai H.**
499 2003. Crystal structure of extended-spectrum β -lactamase Toho-1: insights into the molecular
500 mechanism for catalytic reaction and substrate specificity expansion. *Biochem. J.* **42**:10634-
501 10643.
- 502 45. **Totir MA, Padayatti PS, Helfand MS, Carey MP, Bonomo RA, Carey PR, van den Akker F.**
503 2006. Effect of the inhibitor-resistant M69V substitution on the structures and populations of
504 trans-enamine β -lactamase intermediates. *Biochem.* **45**:11895-11904.
- 505 46. **Belaouaj A, Lapoumeroulie C, Canica MM, Vedel G, Nevot P, Krishnamoorthy R, Paul G.**
506 1994. Nucleotide sequences of the genes coding for the TEM-like β -lactamases IRT-1 and IRT-2
507 (formerly called TRI-1 and TRI-2). *FEMS Microbiol. Lett.* **120**:75-80.
- 508 47. **Giakkoupi P, Tzelepi E, Legakis NJ, Tzouvelekis LS.** 1998. Substitution of Arg-244 by Cys or
509 Ser in SHV-1 and SHV-5 β -lactamases confers resistance to mechanism-based inhibitors and
510 reduces catalytic efficiency of the enzymes. *FEMS Microbiol. Lett.* **160**:49-54.
- 511 48. **Power P, Mercuri P, Herman R, Kerff F, Gutkind G, Dive G, Galleni M, Charlier P,**
512 **Sauvage E.** 2012. Novel fragments of clavulanate observed in the structure of the class A β -
513 lactamase from *Bacillus licheniformis* BS3. *J. Antimicrob. Chemother.* **67**:2379-2387.
- 514 49. **Ruggiero M, Sauvage E, Troncoso F, Curto L, Galleni M, Power P, Gutkind G.** 2012.
515 Mutations in R220 in PER-2 β -lactamase resulting in a decreased susceptibility to inhibitors also
516 impact in the catalytic activity towards substrates, abstr C1-1206., p 134. Abstr. 52nd Intersci.
517 Conf. on Antimicrob. Agents and Chemother., San Francisco, CA, USA. American Society for
518 Microbiology, Washington, DC
- 519
- 520
- 521

522 **Figure legends:**

523

524 **Figure 1:** Amino acid sequence alignment of PER-2 and other class A β -lactamases for which
525 the crystallographic structure has been determined, using the Ambler's residue numbering.
526 Location of α helices and β sheets is indicated in the upper side (taken from the PDB file), and
527 relative solvent accessibility in the bottom (black: highly accessible; grey: poorly accessible;
528 white: hidden or non-accessible). Esprint (<http://esprint.ibcp.fr/ESPrint/ESPrint/>) was used for
529 making the figure.

530

531 **Figure 2:** (a) Overall structure of PER-2 β -lactamase, showing the location of the main motifs of
532 the active site (pink), the unique Ω loop (orange), and the three insertions (compared to TEM-1).
533 (b) Detail of the four-residues insertion in PER-2 (pink) that creates an expanded loop between
534 β 3 and β 4 strands, widening the active site's entrance (orange: TEM-1; green: TOHO-1). (c)
535 Comparison between the singular *trans* bond between Glu166-Ala167 and hydrogen bonds with
536 Asp136 in PER-2 (pink), and the normally *cis* bond between Glu166-Pro167 (and hydrogen
537 bonds with Asn136) found in other class A β -lactamases like TOHO-1 (green). All distances are
538 in angstroms (\AA).

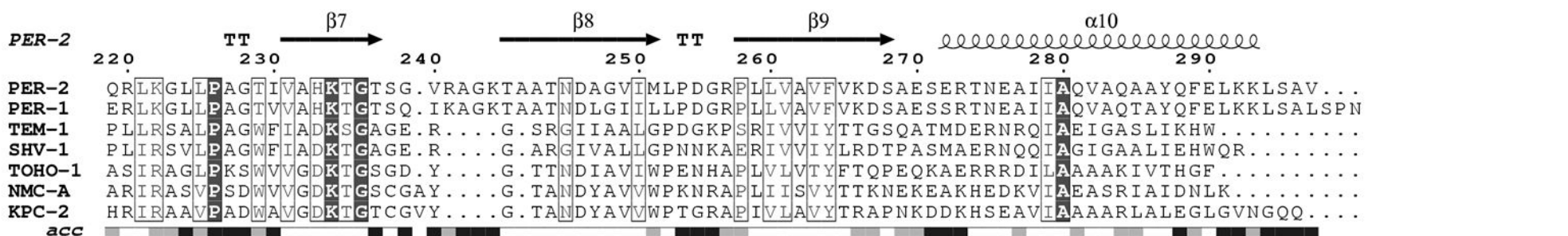
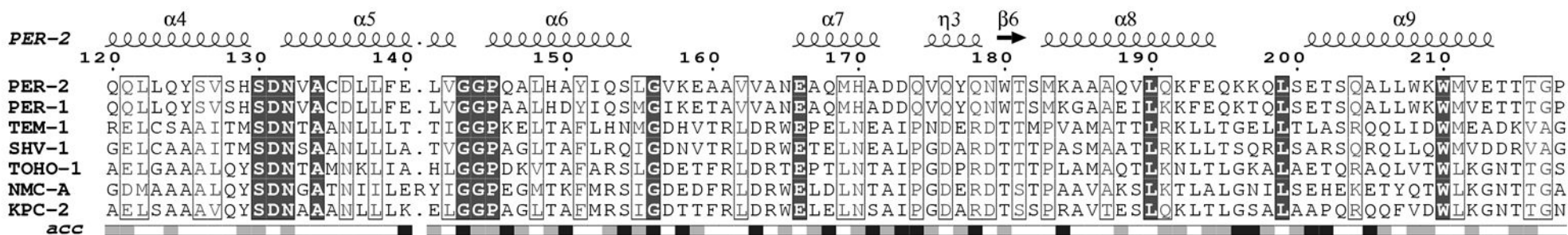
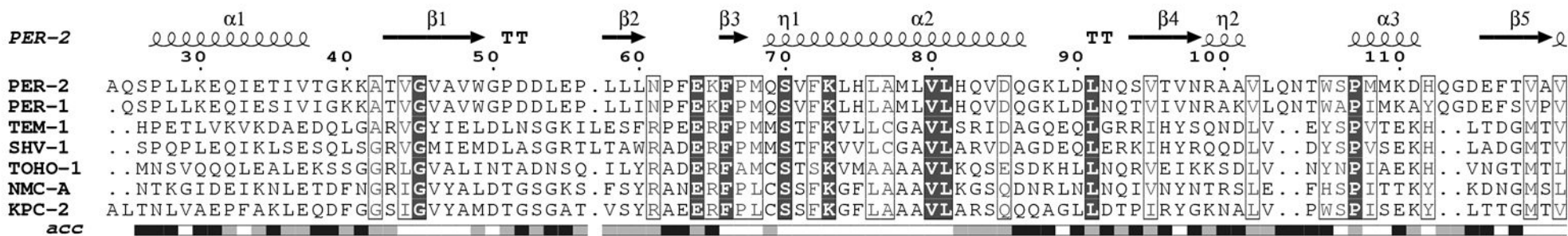
539

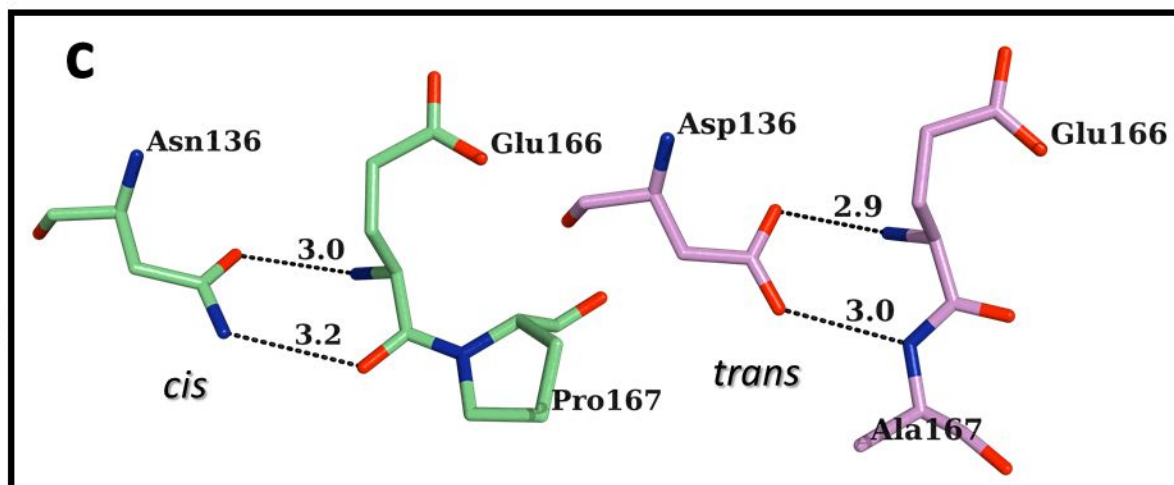
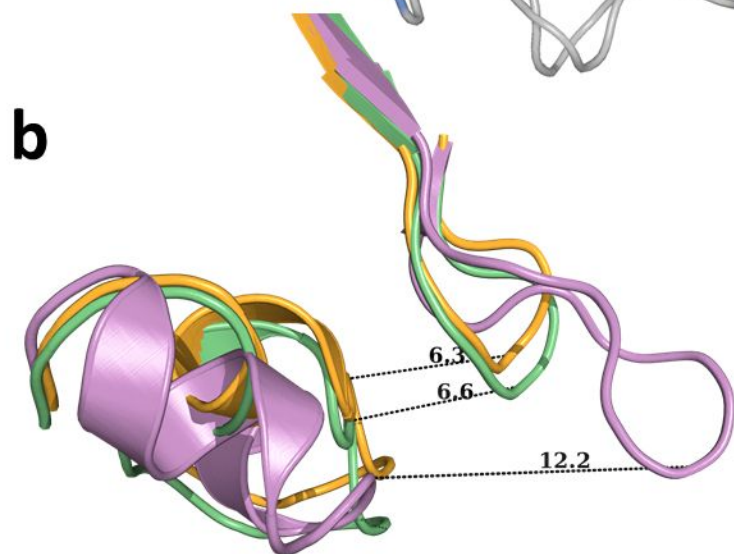
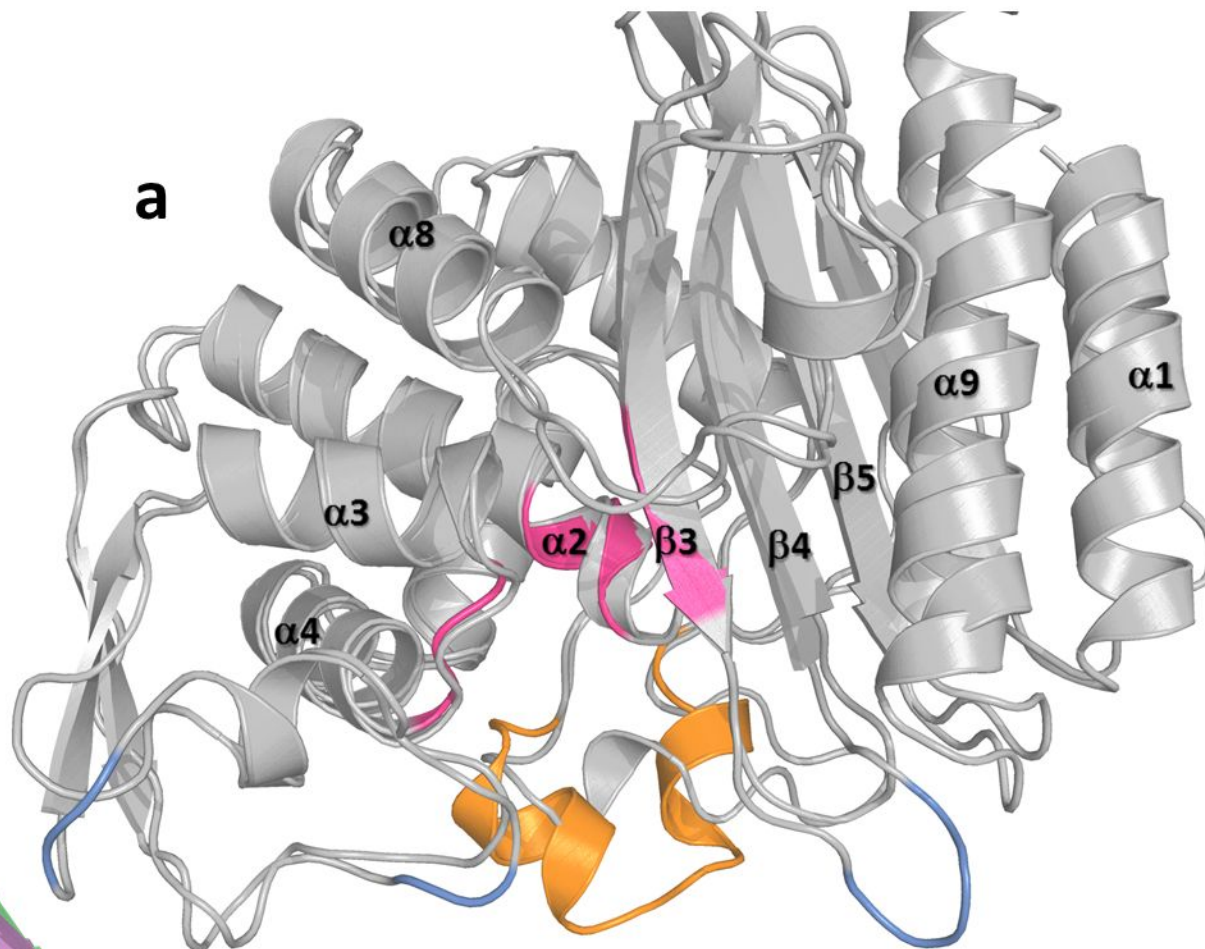
540 **Figure 3:** Detailed view of the structure of active site of PER-2 β -lactamase. (a) $2F_0 - F_c$ map
541 contoured at 1.5σ is shown in grey around the most important amino acid residues within the
542 active site; oxyanion water molecule is shown as a green sphere, and additional water molecules
543 in orange (see text for details). (b) Comparative active site organization of PER-2 (pink) and
544 PER-1 (cyan), indicating the main hydrogen bonds (black dashed lines) implicated in the

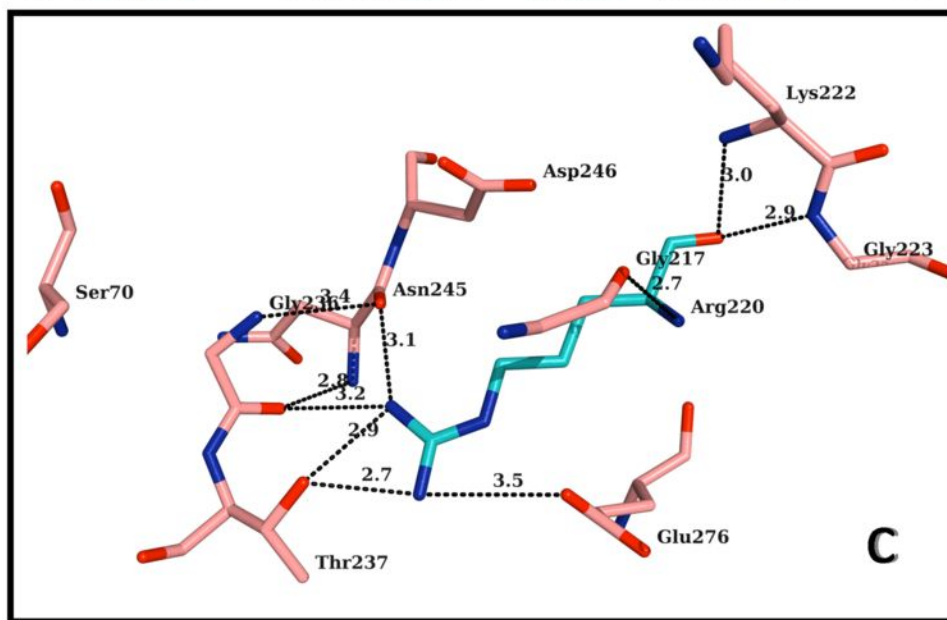
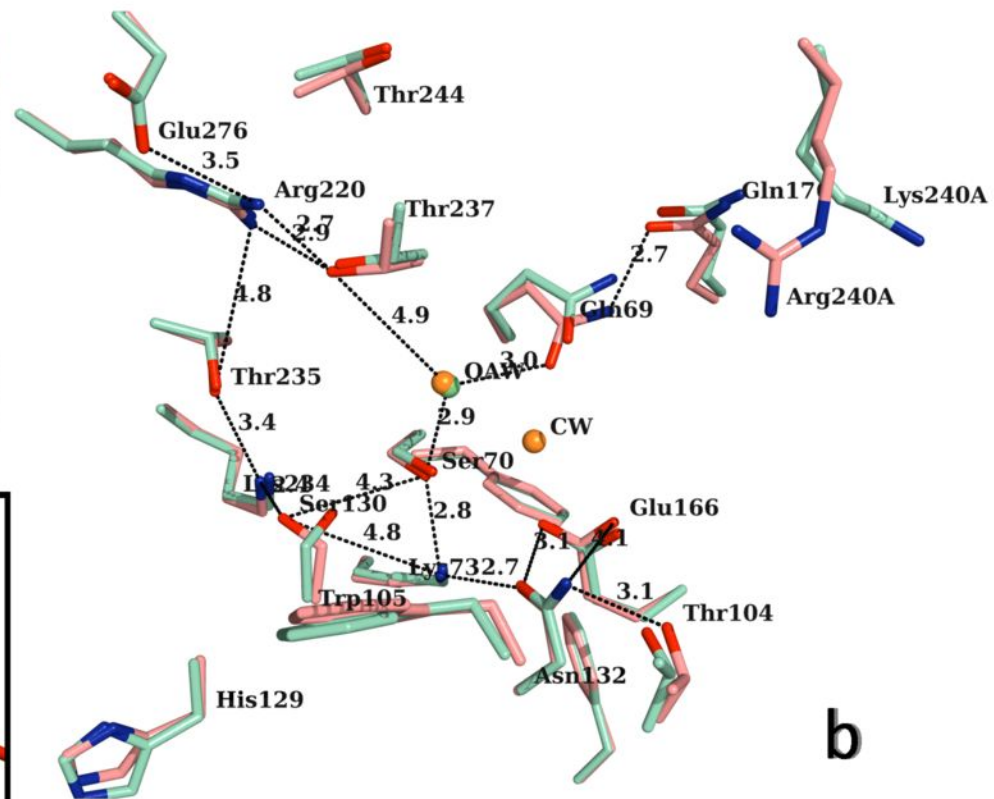
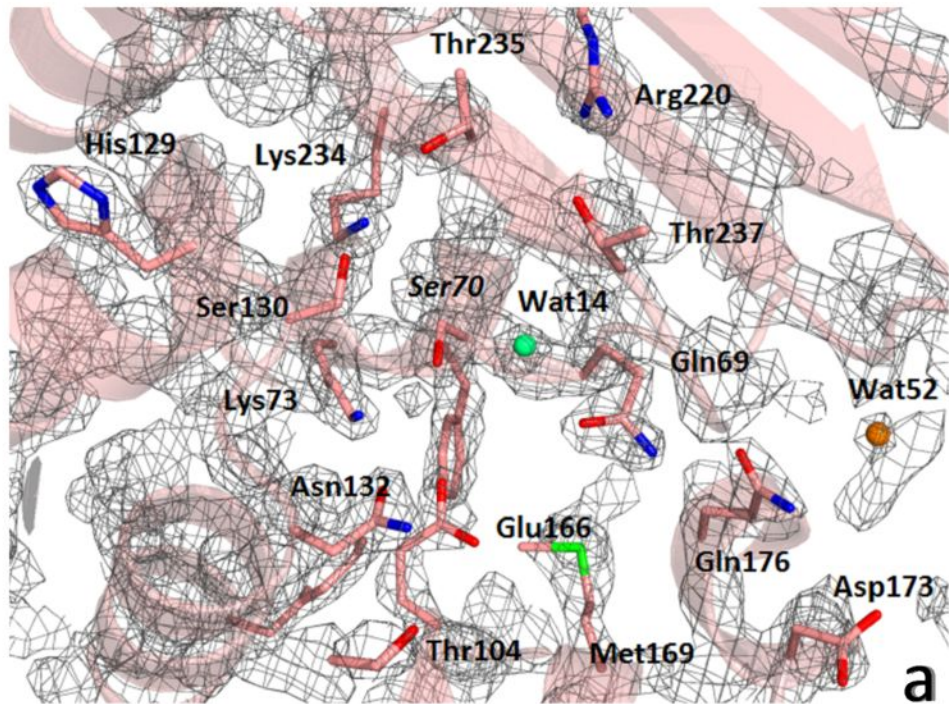
545 stabilization of the active site of PER-2, including the oxyanion water molecules (OAW; green
546 for PER-2 and orange for PER-1) and the catalytic water of PER-1 (CW; orange), and the
547 network “Ser70-Gln69-Wat14-Thr237-Arg220” (see text for details); for visual convenience,
548 only the hydrogen bonds for PER-2 were shown. (c) Position and occupancy of Arg220 in PER-
549 2, allowing the creation of a unique network of hydrogen bonds with neighboring residues like
550 Gly236, Thr237, Asn245 and Glu276, among others; Ser70 is shown as reference. Other color
551 references: oxygen (red), nitrogen (blue), sulfur (green). All distances are in angstroms (Å).

552

553 **Figure 4:** (a) Detailed view of the active site of TOHO-1 in association with cefotaxime (left),
554 indicating the main hydrogen bonds interactions (PDB entry: 1IYO), and simulated modeling of
555 PER-2 and the probable positioning of cefotaxime within the active site (right), suggesting the
556 putative most favorable hydrogen bonds and involvement of residues like Gln69, Thr237 and
557 Arg240A in the stabilization of the oxyimino-cephalosporin molecule. (b) Active site of TOHO-
558 1 in complex with acylated ceftazidime (left), indicating the main hydrogen bonds (PDB entry:
559 2ZQD), compared to a simulated model of PER-2 and its probable association with ceftazidime
560 (right), showing the predicted positioning of the molecule and the hydrogen bonds interactions
561 (black: bonds having regular distances; yellow: probably occurring bonds depending on the
562 rotameric conformations of the involved residues). All distances are in angstroms (Å). See text
563 for details.







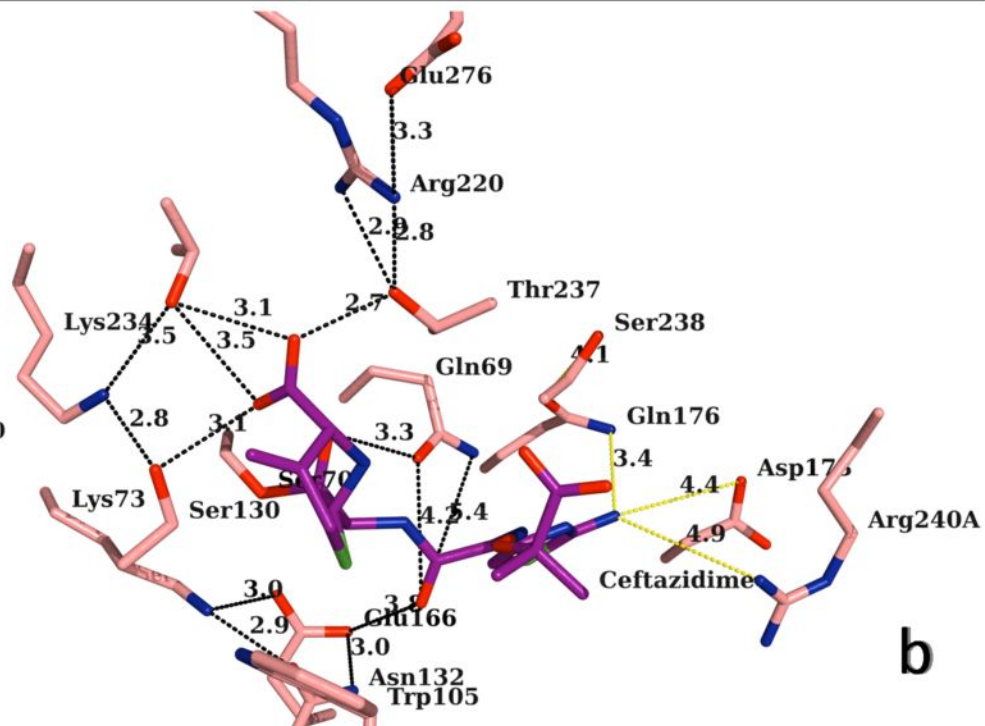
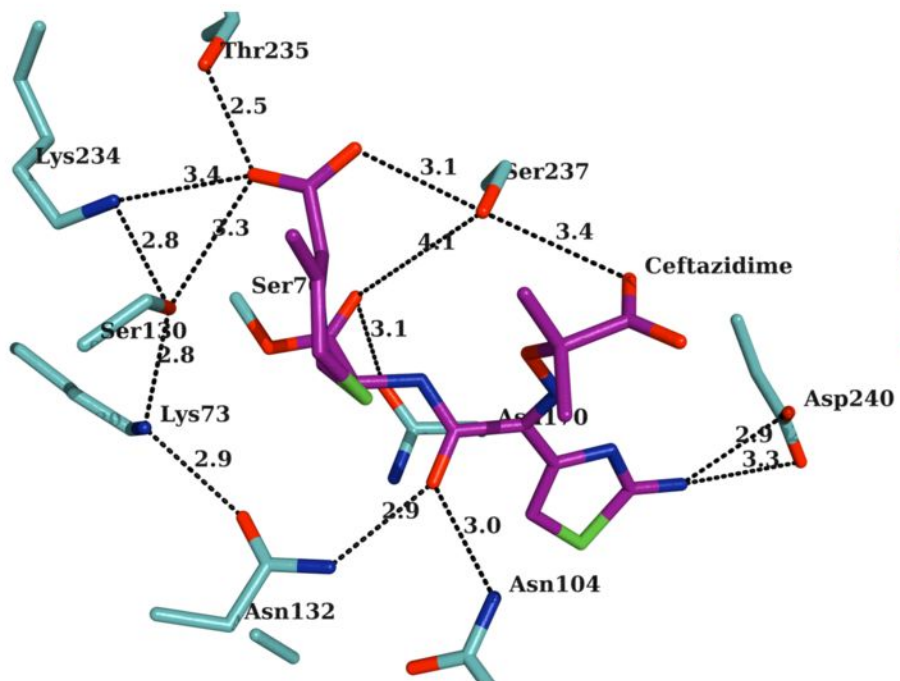
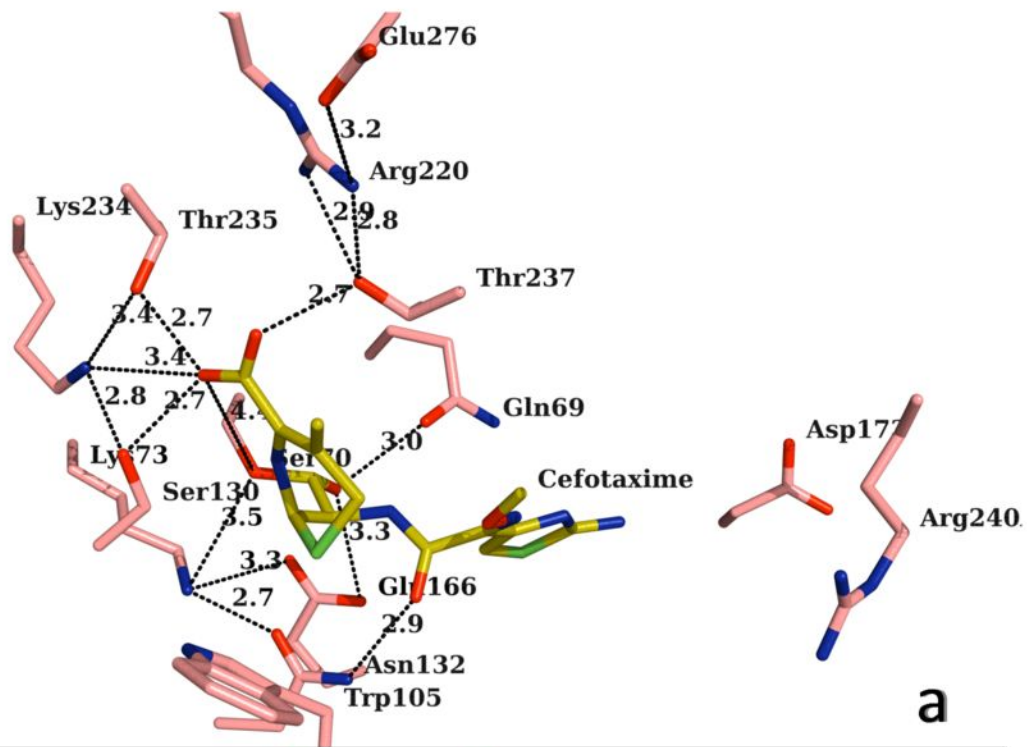
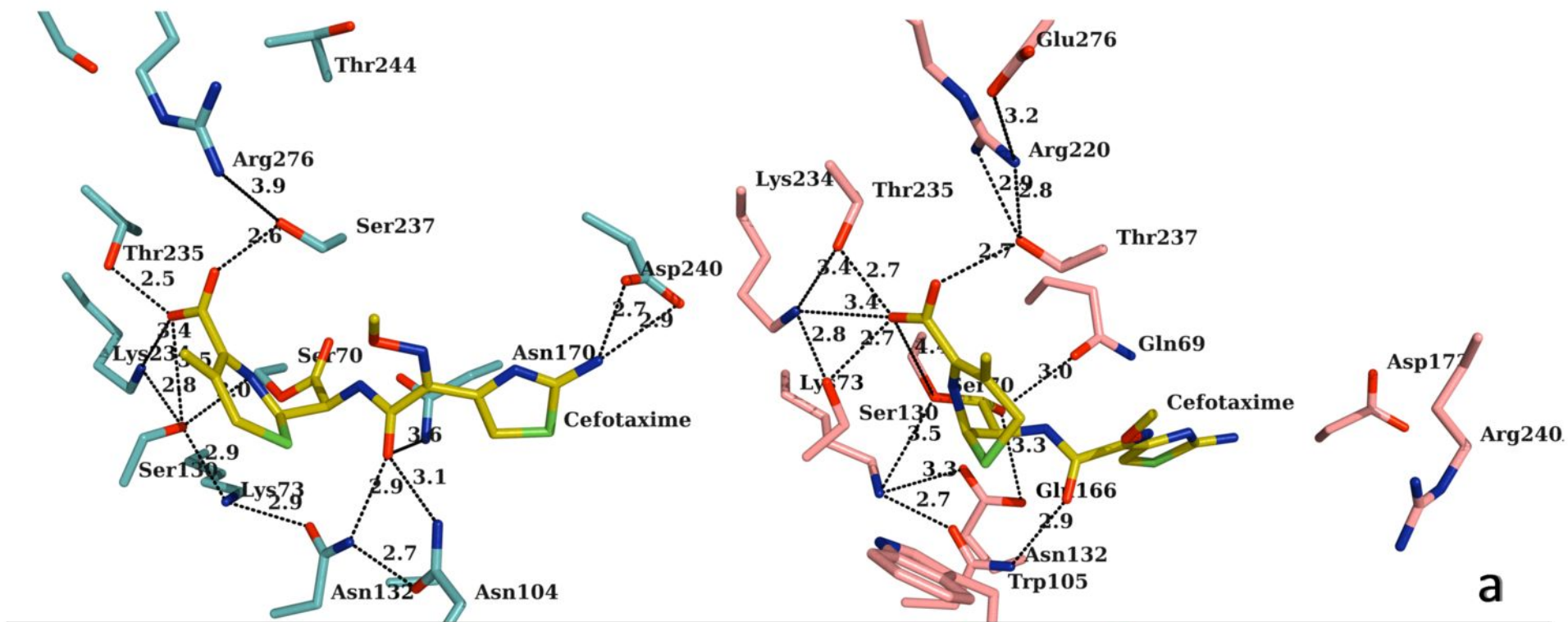


Table 1. Data collection, diffraction and phasing statistics for native PER-2 β -lactamase

Crystal	Native PER-2		
PDB code	4D2O		
<u>Data collection:</u>			
Space group	P 1 21 1		
Cell parameters (\AA)	a = 41.48	b = 83.88	c = 68.94
	$\alpha = 90.00$	$\beta = 103.92$	$\gamma = 90.00$
Subunits/asu	2		
Resolution range (\AA)	41.94 - 2.20 (2.32 – 2.20) ^a		
Total number of reflections	159,256		
Number of unique reflections	23,354 (3,390)		
R_{merge} (%) ^b	14.5 (65.0)		
Redundancy	6.8 (6.9)		
Completeness (%)	100 (100)		
Mean $I/\sigma(I)$	10.5 (3.1)		
<u>Refinement:</u>			
Resolution range	33.46 – 2.20		
No. of protein atoms	4,407		
Number of water molecules	152		
R_{cryst} (%)	19.44		
R_{free} (%)	23.97		
RMS deviations from ideal stereochemistry:			
Bond lengths (\AA)	0.013		

Bond angles (°)	1.619
Planes (Å)	0.007
Chiral center restraint (Å ³)	0.105
Mean B factor (all atoms) (Å ²)	29.2
Ramachandran plot:	
Favored region (%)	97.4
Allowed regions (%)	2.6
Outlier regions (%)	0.0

^a Data in parentheses are statistics for the highest resolution shell

^b RMS: Root-mean square

Table 2. Root-mean square deviations (in Å) between secondary structures and conserved motifs of PER-2 and other class A β -lactamases.

	Complete	SXXK motif	SDN motif	KTG motif	Ω loop
PER-1	0.619	0.116	0.128	0.016	0.220
TEM-1	1.810	0.118	0.086	0.081	3.453
SHV-1	1.894	0.182	0.048	0.033	3.308
TOHO-1	1.629	0.040	0.025	0.070	3.360
KPC-2	1.841	0.171	0.057	0.057	3.408